A NON PARAMETRIC MIXED-EFFECT MODEL FOR POPULATION ANALYSIS: APPLICATION TO ALZHEIMER'S DISEASE DATA

Juan David Ospina[a,b,d], *Oscar Acosta*[a,b], *Renaud de Crevoisier*[a,b,c], *Juan Carlos Correa*[d]
Pascal Haigron[a,b] and the Alzheimer's Disease Neuroimaging Initiative

[a] INSERM, U1099, Rennes, F-35000, France;
[b] Université de Rennes 1, LTSI, Rennes, F-35000, France;
[c] Département de Radiothérapie, Centre Eugène Marquis, Rennes, F-35000, France;
[d] School of Statistics, Universidad Nacional de Colombia, Campus Medellín, Colombia

ABSTRACT

In population analysis, the images of different groups can be compared to locate the effects of a particular disease or treatment and also to generate biomarkers that help in the diagnosis process. Voxel-Based Morphometry (VBM) is a set of widely extended techniques to compare groups of images. VBM involves image normalization, image smoothing, statistical map generation and correction for hypothesis testing. In this paper, we propose the use of a nonparametric mixed-effect model to study Alzheimer's Disease (AD). The proposed method can handle covariates and through the integration of the smoothing and statistical map generation, individual specificities can be controlled. Moreover, it allows the reconstruction of the typical shapes for each group and it can be advantageously used as another VBM implementation.

***Index Terms*—** Statistical analysis of populations, Voxel-based-morphometry, Alzheimer's disease, nonparametric mixed-effects models

1. INTRODUCTION

The problem of assessing differences between groups through the comparison of images is a common practice in medical image analysis. For instance, in neuro degenerative diseases, as Alzheimer's disease (AD), is relevant to quantify the modifications in the brain anatomy and physiology due to the pathology, when comparing to healthy elderly individuals. This has been done, among others, by assessing the decreasing in white matter (WM) concentration [1] or the change in the cortical thickness [2]. This problem has been tackled by the statistical voxel-based methods [3], which uses normalized data to highlight morphological differences across a population as in Voxel-Based Morphometry (VBM) or takes advantage of the deformation resulting in the registration process, such as in Tensor-Based Morphometry (TBM) [4]. Although VBM was born in the neuroimaging domain, it is not restricted to this field. In [5] and [6], authors use VBM to study dose distribution patterns in prostate cancer treatment with radiotherapy. After mapping the dose distribution images against the same template, voxel-based statistics were used to determine the differences in the irradiation patterns in patients presenting some side-effect. In this paper the problem of assessing differences among images of individuals is addressed. It is assumed that images are normalized towards a stereotaxic coordinate system.

In VBM analysis, voxel-based computations are performed to produce statistics that are used later to infer the voxel characteristics. For example, a two-sample t-test can be used to identify if the intensity at a specific voxel is higher for a given group of subjects. Obviously, this implies the verification of the required assumptions before drawing reliable conclusions. In presence of confounding factors, researchers can use a general linear model (glm) to isolate the group effect [3]. The simplest case is when voxel intensities are assumed to come from a Gaussian distribution. Under this assumption, calculations are straightforward and rules to reject the statistical hypothesis are clear.

Smoothing is one of the ways to deal with the lack of normality. By smoothing, each voxel becomes the weighted average of a neighborhood. Thus, under some assumptions the Central Limit Theorem allows to model the voxel distribution as Gaussian [3]. The smoothing step involves two decisions: the shape and bandwidth of the kernel. It has been shown that the bandwidth choice is a critical one [9]. However, smoothing and statistical modeling can be performed in the same step if the nonparametric framework is assumed. This is shown in the literature concerning with nonparametric regression [10]. One of the advantages of the nonparametric framework is that it provides criteria for bandwidth selection. It also takes into account the "smooth" nature of the data under consideration. In this paper it is shown how smoothing can be used to model intra variability without having several images from the same individual, as in functional MRI (fMRI). Then, inference in the nonparametric regression takes advantage of the smoothing [10].

Nonparametric regression techniques have experienced a fast growing with increasing of available computation power. In particular this work exploits the nonparametric mixed-effect model, developed for longitudinal studies. The Nonparametric Mixed-Effects (NPME) model was firstly proposed in [11]. Nevertheless, the mixed-effects (ME) model has been used in VBM to handle intra subject variability in the time domain as in [12, 13, 14]. In [15], with a straightforward reformulation of the nonparametric ME model in the spatial domain, we showed that it could be advantageously applied to perform voxel-based group comparison. The formulation presented herein still relies on the work by [11] and on the adaption done in [15] but, in addition, it is shown how to handle other covariates rather than the group effect.

Data used in the preparation of this article were obtained from the Alzheimer's Disease Neuroimaging Initiative (ADNI) database (`adni.loni.ucla.edu`). The primary goal of ADNI has been to test whether serial magnetic resonance imaging (MRI), positron emission tomography (PET), other biological markers, and clinical and neuropsychological assessment can be combined to measure the progression of mild cognitive impairment (MCI) and early Alzheimer's disease (AD). For up-to-date information, see `www.adni-info.org`.

2. THE NONPARAMETRIC MIXED-EFFECTS MODEL

In this section the Nonparametric Mixed-Effects Model (NPME) is presented. Assume there are n registered images from n different and independent individuals which can be classified either in a group of interest, say T, or its complement, say T^C. Let $f_i(\mathbf{x})$ represents the intensity at voxel $\mathbf{x}$ for the i-th individual and suppose that it can be expressed using an additive model as in eq. (1),

$$f_i(\mathbf{x}) = m(\mathbf{x}) + g(\mathbf{x})\,1_{\{i\in T\}} + A_i a(\mathbf{x}) + e_i(\mathbf{x}) + \varepsilon_i(\mathbf{x}), \tag{1}$$

where $m(\mathbf{x})$, $g(\mathbf{x})$, $a(\mathbf{x})$ and $e_i(\mathbf{x})$ are smooth functions and $\varepsilon_i(\mathbf{x})$ is a random error. $1_{\{i\in T\}}$ is one if the i-th individual belongs to group T and it is zero otherwise. The term $m(\mathbf{x}) + g(\mathbf{x})$ represents the mean of the group T, and $m(\mathbf{x})$ the mean of the group T^C. The term $a(\mathbf{x})$ represents the localized effect of the covariate A (scalar). Further, $e_i(\mathbf{x})$ is the deviation of the i-th individual from the corresponding mean of its group and it is assumed random from the population perspective. Because this kind of model is composed of population and individual features, it has been referred to in the literature as a *mixed-effects model*. Moreover, let $f_e(\mathbf{t})$ the probability density function (pdf) of $e_i(\mathbf{x})$ and $f_\varepsilon(t)$ be the pdf of $\varepsilon_i(\mathbf{x})$. Assuming that $e_i(\mathbf{x})$ and $\varepsilon_i(\mathbf{x})$ are independent, the unconditional pdf of $f_i(\mathbf{x})$ can be expressed as in eq. (2),

$$f_\varepsilon\left(t - \left[m(\mathbf{x}) + g(\mathbf{x})\,1_{\{i\in T\}} + A_i a(\mathbf{x}) + e_i(\mathbf{x})\right]\right) \times f_e(t). \tag{2}$$

It has to be noted that, although for a single individual i, conditioned with respect to himself, the function $e_i(\cdot)$ is deterministic; from the whole population perspective, this is quite a random feature.

Assume that all the functions in eq. (1) admit a first order approximation around $\mathbf{x_0}$. In addition let $\boldsymbol{\beta}_m$, $\boldsymbol{\beta}_g$, $\boldsymbol{\beta}_a$ and $\mathbf{b_i}$, vectors such that, for instance, $\boldsymbol{\beta}_m = \left[\; m(\mathbf{x}_0) \quad \nabla m^T(\mathbf{x}_0) \;\right]^T$ and $\mathbf{b}_i = \left[\; e_i(\mathbf{x}_0) \quad \nabla e_i^T(\mathbf{x}_0) \;\right]^T$. Finally, if $\Delta_{\mathbf{x}} = \left[\; 1 \quad (\mathbf{x}-\mathbf{x}_0)^T \;\right]^T$, then $f_i(\mathbf{x})$ can be approximated as in eq. (3),

$$f_i(\mathbf{x}) = \Delta_{\mathbf{x}}^T\boldsymbol{\beta}_m + 1_{\{i\in T\}}\Delta_{\mathbf{x}}^T\boldsymbol{\beta}_g + A_i\Delta_{\mathbf{x}}^T\boldsymbol{\beta}_a + \Delta_{\mathbf{x}}^T\mathbf{b}_i + \varepsilon_i(\mathbf{x}). \tag{3}$$

Suppose now that the d image voxels are indexed as $\mathbf{x}_{s_1}$, $\mathbf{x}_{s_2}$, ..., $\mathbf{x}_{s_d}$. Thus, $n\times d$ points are available to estimate the model for all the individuals. For each individual the response vector around $\mathbf{x}_{s_j}$ is defined as $\mathbf{Y_i} = \left[\; f_i(\mathbf{x}_{s_1}) \quad \ldots \quad f_i(\mathbf{x}_{s_d}) \;\right]^{\mathbf{T}}$, that in matrix notation can be expressed as in eq. (4),

$$\mathbf{Y}_i = \mathbf{X}_i\boldsymbol{\beta} + \mathbf{X}^*\mathbf{b}_i + \boldsymbol{\varepsilon}_i, \tag{4}$$

with $\mathbf{X}^* = \begin{bmatrix} \Delta_{j1}^T \\ \vdots \\ \Delta_{jd}^T \end{bmatrix}$, $\mathbf{X}_i = \left[\; \mathbf{X}^* \quad 1_{\{i\in T\}}\mathbf{X}^* \quad A_i\mathbf{X}^* \;\right]$, $\boldsymbol{\beta} = \left[\; \boldsymbol{\beta}_m^T \quad \boldsymbol{\beta}_g^T \quad \boldsymbol{\beta}_a^T \;\right]^T$ and $\Delta_{jk} = \left[\; 1 \quad (\mathbf{x}_k - \mathbf{x}_j)^T \;\right]^T$. Moreover, by concatenating the vectors and matrix as $\mathbf{Y} = \left[\; \mathbf{Y}_1^T \quad \ldots \quad \mathbf{Y}_n^T \;\right]^T$, $\mathbf{X} = \begin{bmatrix} \mathbf{X}_1 \\ \vdots \\ \mathbf{X}_n \end{bmatrix}$, $\mathbf{Z} = \begin{bmatrix} \mathbf{X} & & \\ & \ddots & \\ & & \mathbf{X} \end{bmatrix}$ and $\mathbf{b} = \left[\; \mathbf{b}_1^T \quad \ldots \quad \mathbf{b}_n^T \;\right]^T$, the model for all the individuals can be expressed as in eq. (5),

$$\mathbf{Y} = \mathbf{X}\boldsymbol{\beta} + \mathbf{Z}\mathbf{b} + \boldsymbol{\varepsilon}. \tag{5}$$

The vector $\boldsymbol{\varepsilon}$ is the evident concatenation of the $\boldsymbol{\varepsilon}_i$s vectors, which contain the errors for the individuals at each voxel. The model in eq. (5) has two random terms: the individual specificities represented in vector $\mathbf{b}$ that models intra-individual variability; the other is the error vector $\boldsymbol{\varepsilon}$ which model inter-individuals variability. This model has the form of a linear mixed-effects models (LME) and it can be estimated using Maximum Likelihood (ML) or Restricted ML (RML) as it is shown in [18]. The estimate of $\boldsymbol{\beta}$, $\hat{\boldsymbol{\beta}}$, and the prediction for $\mathbf{b}$, $\hat{\mathbf{b}}$, contain the estimates of $m(\mathbf{x}_{s_j})$, $g(\mathbf{x}_{s_j})$, $a(\mathbf{x}_{s_j})$, and $e_i(\mathbf{x}_{s_j})$, $i = 1,\ldots,n$. In order to weight the contribution of the voxel $\mathbf{x}_{s_k}$ when estimating the terms around $\mathbf{x}_{s_j}$ a kernel $k_h(\cdot) = \frac{1}{h}k\left(\frac{\cdot}{h}\right)$ is used. The parameter h is called the bandwidth. The weighing matrix is defined as $\mathbf{K}_h = diag\left(\mathbf{K}_{jh},\ldots,\mathbf{K}_{jh}\right)$ (a $nd\times nd$ matrix), where

$$\mathbf{K}_{jh} = diag\left(k_h\left(\left\|\mathbf{x}_{s_1} - \mathbf{x}_{s_j}\right\|\right),\ldots,k_h\left(\left\|\mathbf{x}_{s_d} - \mathbf{x}_{s_j}\right\|\right)\right)$$

is a $d\times d$ matrix a kernel function with bandwidth h. The model to be estimated is the one of eq. (5) pre-multiplying both sides by $\mathbf{K}_h^{1/2}$. Assuming that $\mathbf{b}$ and $\boldsymbol{\varepsilon}$ are both independent Gaussian vector with covariance matrix D and V, respectively, the local joint weighted log-likelihood can be written as in eq. (6),

$$l(\boldsymbol{\beta},\mathbf{b}|\mathbf{Y}) = -\frac{1}{2}\left(\mathbf{r^T}\mathbf{V}_h\mathbf{r} + \mathbf{b}^T\mathbf{D}^{-1}\mathbf{b}\right) + C, \tag{6}$$

with $\mathbf{r} = \mathbf{Y} - \mathbf{X}\boldsymbol{\beta} - \mathbf{Z}\mathbf{b}$, $\mathbf{V}_h = \mathbf{K}_h^{1/2}V^{-1}\mathbf{K}_h^{1/2}$ and $C = \log|V| + \log|D| - \frac{nd+4n}{2}\log(2\pi)$. By minimizing (6), the Local Polinomial ME (LPME) estimates are obtained [10, 19]. Additionally, this minimization should be done for each voxel $\mathbf{x}_{s_j}$ in order to have the corresponding estimates $\hat{m}(\mathbf{x}_{s_j})$, $\hat{g}(\mathbf{x}_{s_j})$, $\hat{a}(\mathbf{x}_{s_j})$. In this work, the estimates divided by their corresponding standard errors are used as statistics to assess the significance of the estimates. The distribution of those statistics is assumed standard normal. The standard errors are taken from the estimated fixed-effects covariance matrix.

3. APPLICATION TO AD STUDY

In this study, we investigated the ability of our method to detect differences in gray matter (GM) between a population of healthy elderly (HE) individuals, and Alzheimer's disease patients (AD) and compared the results with SPM8. From the ADNI database we selected 22 AD patients (mean age at baseline 75.58 $\pm$ 5.69, mean MMSE 23.41 $\pm$ 1.79), a first group with 22 HE controls (mean age at baseline 74.83$\pm$ 5.49, mean MMSE 28.71 $\pm$ 1.45) and a second group with 22 HE controls (mean age at baseline 70.82$\pm$ 3.11, mean MMSE 28.91 $\pm$ 1.34). All images were identified in the ADNI database as best in terms of the quality ratings. All patients were imaged on a 1.5 T scanner with in-plane resolution of 0.94 $\times$ 0.94 mm, 1.25 $\times$ 1.25 mm and 1.30 $\times$ 1.30 mm, and slice thickness of 1.2 mm (Detailed information about MR acquisition procedures is available at the ADNI website www.adni-info.org). All images were corrected for gradient non-linearity distortion, intensity non-uniformity, and were scaled for gradient drift using the phantom data.

The MRI were segmented and normalized towards a stereotaxic coordinate system using SPM8. Modulated probability maps were then used as input in both, our method and in VBM as it is performed by SPM.

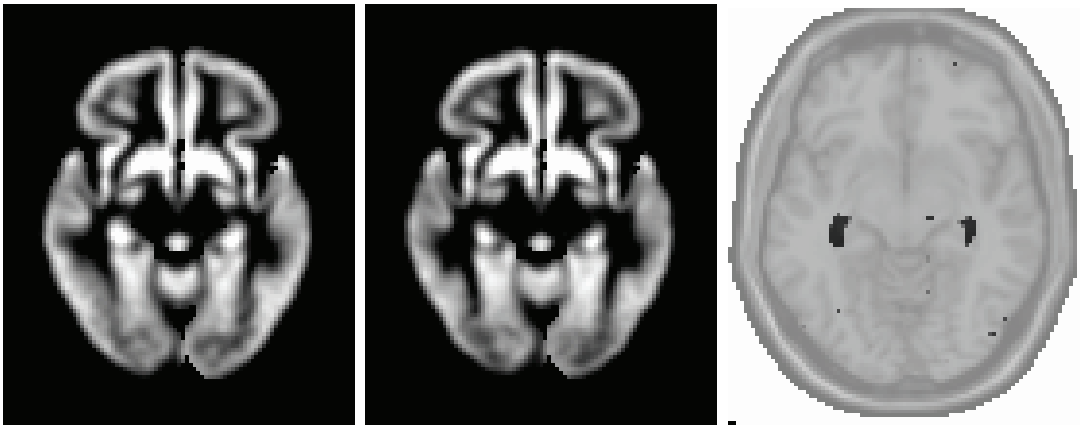
When assessing the localized effects of the AD using the first group of HE controls and the AD patients, it is expected that the age has not an important effect in the analysis. However, when using the second group of HE controls and the AD patients the contrary is

	NPME				SPM8			
	Without age		With age		Without age		With age	
Structure	P<0.05	P<0.001	P<0.05	P<0.001	P<0.05	P<0.001	P<0.05	P<0.001
Hipp L	59.30%	25.21%	58.16%	26.45%	72.62%	20.76%	70.76%	24.59%
Hipp R	55.70%	28.36%	54.49%	27.25%	70.33%	25.43%	68.82%	23.71%
ITG L	18.82%	1.97%	17.78%	1.85%	30.33%	0.58%	27.90%	0.49%
ITG R	11.48%	0.36%	10.47%	0.38%	23.84%	0.08%	22.53%	0.05%

Table 1. Estimated percentage of volume affected by the AD. Results of analysis performed with group 1 of HE vs. AD.

	NPME				SPM8			
	Without age		With age		Without age		With age	
Structure	P<0.05	P<0.001	P<0.05	P<0.001	P<0.05	P<0.001	P<0.05	P<0.001
Hipp L	78.20%	55.58%	58.47%	23.04%	74.90%	37.19%	55.37%	9.61%
Hipp R	64.38%	45.91%	53.78%	27.85%	67.51%	20.48%	56.71%	11.60%
ITG L	35.10%	6.80%	22.05%	2.58%	28.45%	0.15%	24.24%	0.00%
ITG R	30.91%	5.21%	22.14%	1.75%	24.83%	0.05%	38.26%	0.05%

Table 2. Estimated percentage of volume affected by the AD. Results of analysis performed with group 2 of HE vs. AD.



(a) HE control brain. (b) AD brain. (c) $P - values < 0.001$.

Fig. 1. Typical 75 year old individual GM brain models generated with the NPME model and p-value (darkest points correspond to significant values).

expected and modeling the impact of age should affect the results. The effect of the age in GM changes has been studied for example in [20]. There VBM is used to examine the effects of aging on gray matter asymmetry.

Firstly, localized effects of the AD were assessed using the AD and the first group of HE controls. Secondly, the same was performed using the second group of HE controls. In both cases the localized effects were assessed with and without include the age as covariate. Four regions were selected to perform the analysis: the left hippocampus (Hipp L), right hippocampus (Hipp R), left inferior temporal gyrus (ITG L) and right inferior temporal gyrus (ITG R). The percentage of affected volume was calculated as the number of significant voxels within a region divided by the total number of voxels of that region. Two confidence levels were used: 95% (P<0.05) and 99.9% (P<0.001). As the methodologies to perform correction for FPR with the NPME are matter of future research, the uncorrected p-values are used for both methodologies. A symmetric kernel of 8mm Full Width at Half Maximum (FWHM) was used in SPM8 to smooth the images. The same kernel was used in the nonparametric mixed-effects model. The methodology was programmed using R [21]. The experiment results are presented in tables 1 and 2.

4. DISCUSSION

From tables 1 and 2 it can be noticed that the proposed methodology produces consistent results for both HE control groups when modeling the age. As it was expected, when using the first group of controls the impact of modeling the age was not significant. By the contrary, when using the second group of controls the proposed methodology, including the age as covariate, exhibits similar results than when using the first HE controls. The results obtained with SPM8 substantially change depending on the control group.

In addition, it is possible to derive a voxel-based model for the GM. As it is assumed that the random deviations $e_i\left(\mathbf{x}_{s_k}\right)$ are zero-mean normal variables, the expected intensities of GM for typical HE control and AD patients at a given age A, for the $\mathbf{x}_{s_k}$ voxel, can be written as in eq. (7) and (8), respectively,

$$\hat{f}\left(\mathbf{x}_{s_k}\right) = \hat{m}\left(\mathbf{x}_{s_k}\right) + A \times a\left(\mathbf{x}_{s_k}\right), \tag{7}$$

$$\hat{f}\left(\mathbf{x}_{s_k}\right) = \hat{m}\left(\mathbf{x}_{s_k}\right) + \hat{g}\left(\mathbf{x}_{s_k}\right) + A \times a\left(\mathbf{x}_{s_k}\right). \tag{8}$$

Moreover, using the eq. (7) and (8) it is possible to reconstruct the typical brains for HE and AD patients. Figures 1(a) and 1(b) depict this reconstruction for two 75 year old patients. Figure 1(c) shows the p-value map to assess the differences among the two groups. The interest of doing this type of reconstruction is that for

a new patient, whose diagnose is not known, it would be possible to use those models to identify the one which it has the better correspondence. This could be done applying voxel-wise goodness of fit tests and choosing the model that match better the new patient.

In this work a 8 mm FWHM Gaussian kernel was used. There are several proposals in the literature to chose the optimal bandwidth. Some authors suggest using different bandwidths to estimate fixed and random effects [22]. For such a purpose, bandwidth selection strategies based on cross-validation can be used [19, p. 87]. However, they are computationally expensive to be applied in voxel-wise models and efficient methods should be developed to use a cross-validation bandwidth selection strategy. For instance, the optimal bandwidth could be selected as the one that minimizes the leave-one-patient-out cross-validation error shown in eq. (9),

$$CV\left(h\right) = \frac{1}{n \times d} \sum_{i=1}^{n} \sum_{k=1}^{d} \left(\hat{f}_i^{(h)} \left(\mathbf{x}_{s_k}\right) - f_i \left(\mathbf{x}_{s_k}\right) \right)^2, \quad (9)$$

where $\hat{f}_i^{(h)} \left(\mathbf{x}_{s_k}\right)$ is the estimate of $f_i \left(\mathbf{x}_{s_k}\right)$ using a model estimated without the i-th individual and the bandwidth h. By choosing h in this way, the conclusions will be supported in the fitted model that better describes the population.

Finally, we have shown that the proposed method can be used to perform VBM, but in addition it could allow as well to do classification or to help in the diagnose process. Moreover, using the developed theory for NPME it would be possible to develop methodologies for objective kernel bandwidth selection. Efficient methods to perform voxel-wise goodness of fit tests and kernel bandwidth selection are matter of future works.

5. ACKNOWLEDGMENTS

Data collection and sharing for this project was funded by the Alzheimer's Disease Neuroimaging Initiative (ADNI) (National Institutes of Health Grant U01 AG024904). ADNI is funded by the National Institute on Aging, the National Institute of Biomedical Imaging and Bioengineering, and through generous contributions

6. REFERENCES

[1] Y. Hirata, H. Matsuda, *et al*, "Voxel-based morphometry to discriminate early alzheimer's disease from controls," *Neuroscience Letters*, vol. 382, no. 3, pp. 269 – 274, 2005.

[2] O. Acosta, P. Bourgeat, *et al*, "Automated voxel-based 3d cortical thickness measurement in a combined lagrangian-eulerian pde approach using partial volume maps," *Medical Image Analysis*, vol. 13, no. 5, pp. 730 – 743, 2009, Includes Special Section on the 12th International Conference on Medical Imaging and Computer Assisted Intervention.

[3] K.J. Friston, A.P. Holmes, *et al*, *Human Brain Mapping*, chapter Statistical Parametric Maps in Functional Imaging: A General LInear Approach, pp. 189–210, 1995.

[4] J. Ashburner and K.J. Friston, "Nonlinear spatial normalizatioon using bbasis functions," *in Human Brain Mapping*, vol. 7, pp. 254–266, 1999.

[5] W.D. Heemsbergen, M.S. Hoogeman, *et al*, "Increased risk of biochemical and clinical failure for prostate patients with a large rectum at radiotherapy planning: Results from the dutch trial of 68 gy versus 78 gy," *International Journal of Radiation Oncology*Biology*Physics*, vol. 67, no. 5, pp. 1418 – 1424, 2007.

[6] M.G. Witte, W.D. Heemsbergen,*et al*, "Relating dose outside the prostate with freedom from failure in the dutch trial 68 gy vs. 78 gy," *International Journal of Radiation Oncology*Biology*Physics*, vol. 77, no. 1, pp. 131 – 138, 2010.

[7] G.R. Ridgway, S. M.D. Henley, *et al*, "Ten simple rules for reporting voxel-based morphometry studies," *NeuroImage*, vol. 40, no. 4, pp. 1429 – 1435, 2008.

[8] K.J. Worsley, S. Marrett, *et al*, "A unified statistical approach for determining significant voxels in images of cerebral activation," *Human Brain Mapping*, vol. 4, pp. 58–73, 1996.

[9] D.K. Jones, M.R. Symms, *et al*, "The effect of filter size on vbm analyses of dt-mri data," *NeuroImage*, vol. 26, no. 2, pp. 546 – 554, 2005.

[10] H. Wu and J.T. Zhang, "Local polynomial mixed-effects models for longitudinal data," *Journal of American Statistical Association*, vol. 97, pp. 883–897, 2002.

[11] D.R. Hoover, J.A. Rice, *et al*, "Nonparametric smoothing estimates of time-varying coefficient models with longitudinal data.," *Biometrika*, vol. 85, pp. 809–822, 1998.

[12] K.J. Friston, K.E. Stephan, *et al*, "Mixed-effects and fmri studies," *NeuroImage*, vol. 24, pp. 244–252, 2005.

[13] J.A. Mumford and T. Nichols, "Modeling and inference of multisubject fmri data," *Engineering in Medicine and Biology Magazine, IEEE*, vol. 25, no. 2, pp. 42 –51, march-april 2006.

[14] A. Roche, S. Mériaux, *et al*, "Mixed-effects statistics for group analysis in fmri: A nonparametric maximum likelihood approach," *Neuroimage*, vol. 38, pp. 501–510, 2007.

[15] J.D. Ospina, O. Acosta, *et al*, "Spatial nonparametric mixed-effects model with spatial-varying coefficients for analysis of populations," in *MLMI*, 2011, pp. 142–150.

[16] R. Tibshirani and T. Hastie, "Local likelihood estimation," *Journal of the American Statistical Association*, vol. 82, no. 398, pp. 559–567, 1987.

[17] J. Fan, M. Farmen, *et al*, "Local maximum likelihood estimation and inference," *Journal of the Royal Statistical Society: Series B (Statistical Methodology)*, vol. 60, no. 3, pp. 591–608, 1998.

[18] J.C. Pinheiro and D.M. Bates, *Mixed-Effects models in S and S-Plus*, Springer, 1 edition, 2000.

[19] H. Wu and J.T. Zhang, *Nonparametric Regression Methods for Longitudinal Data Analysis*, John Wiley & Sons, Inc., New Jersey, 2006.

[20] H. Takao, O. Abe, *et al*, "Aging effects on cerebral asymmetry: a voxel-based morphometry and diffusion tensor imaging study," *Magnetic Resonance Imaging*, vol. 28, no. 1, pp. 65 – 69, 2010.

[21] R Development Core Team, *R: A Language and Environment for Statistical Computing*, R Foundation for Statistical Computing, Vienna, Austria, 2010, ISBN 3-900051-07-0.

[22] J.A. Rice and B.W. Silverman, "Estimating the mean and covariance structure nonparametrically when the data are curves," *Journal of Royal Statistical Society, Series B*, vol. 57, pp. 253–259, 1991.